Original Article

Radiomic and gEnomic approaches for the enhanced DIagnosis of clear cell REnal Cancer (REDIRECt): a translational pilot methodological study

Francesco Cianflone[1], Dejan Lazarevic[2], Anna Palmisano[3], Giuseppe Fallara[1], Alessandro Larcher[1], Massimo Freschi[4], Giacomo Dell'Antonio[4], Giulia Maria Scotti[2], Marco J. Morelli[2], Anna Maria Ferrara[1], Francesco Trevisani[1], Alessandra Cinque[1], Antonio Esposito[3], Alberto Briganti[1], Carlo Tacchetti[5], Claudio Doglioni[4], Alessandro del Maschio[3], Francesco de Cobelli[3], Roberto Bertini[1], Andrea Salonia[1], Francesco Montorsi[1], Giovanni Tonon[2], Umberto Capitanio[1]

[1]Unit of Urology, Division of Experimental Oncology, Urological Research Institute, IRCCS San Raffaele Scientific Institute, Vita-Salute San Raffaele University, Milan, Italy; [2]Center for Omics Scences, IRCCS San Raffaele Scientific Institute, Milan, Italy; [3]Department of Radiology, Experimental Imaging Centre, IRCCS San Raffaele Scientific Institute, Vita-Salute San Raffaele University, Milan, Italy; [4]Department of Pathology, IRCCS San Raffaele Scientific Institute, Milan, Italy; [5]Unit of Cancer Imaging, Experimental Imaging Centre, IRCCS San Raffaele Scientific Institute, Vita-Salute San Raffaele University, Milan, Italy

Contributions: (I) Conception and design: U Capitanio, G Tonon, D Lazarevic; (II) Administrative support: AM Ferrara; (III) Provision of study materials or patients: A Larcher, D Lazarevic, A Palmisano, M Freschi, G Dell'Antonio, GM Scotti; (IV) Collection and assembly of data: A Larcher, D Lazarevic, A Palmisano, M Freschi, G Dell'Antonio, GM Scotti; (V) Data analysis and interpretation: F Cianflone, A Larcher, D Lazarevic, A Palmisano, M Freschi, G Dell'Antonio, GM Scotti, U Capitanio, G Tonon; (VI) Manuscript writing: All authors; (VII) Final approval of manuscript: All authors.

Correspondence to: Umberto Capitanio. Division of Oncology/Unit of Urology URI, IRCCS Ospedale San Raffaele, Via Olgettina 60, Milan 20132, MI, Italy. Email: capitanio.umberto@hsr.it.

Background: The combination of radiomic and transcriptomic approaches for patients diagnosed with small clear-cell renal cell carcinoma (ccRCC) might improve decision making. In this pilot and methodological study, we investigate whether imaging features obtained from computed tomography (CT) may correlate with gene expression patterns in ccRCC patients.

Methods: Samples from 6 patients who underwent partial nephrectomy for unilateral non-metastatic ccRCC were included in this pilot cohort. Transcriptomic analysis was conducted through RNA-sequencing on tumor samples, while radiologic features were obtained from pre-operative 4-phase contrast-enhanced CT. To evaluate the heterogeneity of the transcriptome, after a 1,000 re-sampling via bootstrapping, a first Principal Component Analyses (PCA) were fitted with all transcripts and a second ones with transcripts deriving from a list of 369 genes known to be associated with ccRCC from The Cancer Genome Atlas (TCGA). Significant pathways in each Principal Components for the 50 genes with the highest loadings absolute values were assessed with pathways enrichment analysis. In addition, Pearson's correlation coefficients among radiomic features themselves and between radiomic features and transcripts expression values were computed.

Results: The transcriptomes of the analysed samples showed a high grade of heterogeneity. However, we found four radiogenomic patterns, in which the correlation between radiomic features and transcripts were statistically significant.

Conclusions: We showed that radiogenomic approach is feasible, however its clinical meaning should be further investigated.

Keywords: Kidney cancer; renal cancer; genomics; radiomics; transcriptomics

Submitted Aug 13, 2021. Accepted for publication Dec 16, 2021.
doi: 10.21037/tau-21-713
View this article at: https://dx.doi.org/10.21037/tau-21-713

Introduction

Clear-cell renal cell carcinoma (ccRCC) is the most common RCC subtype, accounting for almost 70% of all RCC diagnoses (1). Incidence predominates in men, being male-to-female ratio 1.5:1.0, and peaks at age 60–70 years. RCC is the sixth most common cancer for male and eighth for female in US (2). Estimated five-year relative survival is almost 75%, but it is highly heterogenic depending on stage, grade, histology and several cancer and patient features (2). Employing a combined radiomic and genomic approach might improve decision making, as it is currently happening for breast cancer, lung cancer, head and neck cancer (3-5).

In the past years, the molecular characterization of ccRCC has brought to the discover of new genetic pathways, methylation patterns and transcripts (6-9), suggesting possible targets for new therapies which then became the cornerstone of metastatic ccRCC management (10,11). In addition, gene expression clusters have been found to correlate with patients' long-term oncologic outcomes (12,13). However, genetic analyses are rarely used in everyday practice (14).

Radiomics is a new field based on quantitative analysis of radiological images, either computed tomography (CT), magnetic resonance imaging (MRI) or positron emission tomography (PET) (15,16). It has been shown that radiomic patterns may predict patient's long-term oncologic outcomes in different tumours, such as non-small cell lung cancer and glioblastoma (17,18). However, few evidences exist for radiomics in ccRCC and only a few combined radiomic with genomic data (19,20).

The combination of radiomics and genomics might be useful in several steps of the RCC workup: for example, in diagnosis, to define the nature of small renal masses; in active surveillance, to drive the choice toward surveillance or active treatment; in cancer staging, to better stratify aggressiveness of the tumour; in medical treatment choice, to select optimal candidates for adjuvant/first/second line immune/chemotherapies.

Therefore, the aim of this pilot study is to establish a method for radiogenomic characterisation of small ccRCC masses, focusing on the transcriptomic underpinnings of radiomic features. We present the following article in accordance with the MDAR checklist (available at https://tau.amegroups.com/article/view/10.21037/tau-21-713/rc).

Methods

Study population

Six patients diagnosed with ccRCC were randomly selected from a prospective maintained database, according to the following inclusion criteria: age 18–85 years, single monolateral organ-confined non-metastatic renal mass (pT1a-b stage, 5 cm maximum diameter), clear cell histology, no previous diagnosis of renal cancer, complete clinical history, blood and tumour samples collected at the time of surgery and available in our biobank, and availability of a preoperative contrast-enhanced 4-phase multidetector contrast-enhanced computed tomography (MDCT) performed at our Institution. All patients had been submitted to partial nephrectomy.

The study was approved by the institutional ethical board of San Raffaele Hospital in Milan (protocollo No. URI001-2010 RENE - versione 29/08/2007). Informed consent was collected from each patient. The study was conducted in accordance with the principles outlined in the Declaration of Helsinki (as revised in 2013).

Clinical and pathological evaluation

Complete anamnestic and preoperative data were recorded, including age, patient weight and height, body mass index (BMI) estimated glomerular filtration rate (eGFR) and clinical tumour size, defined as the greatest tumour diameter in centimetres on pre-operative imaging. Tumor was staged according to TNM 8th edition, 2017. eGFR was calculated with the Chronic Kidney Disease Epidemiology Collaboration formula for younger patients (<70 years) and with the Berlin Initiative Study formula for older patients (≥70 years). A dedicated experienced genitourinary pathologist re-examined the surgical specimens to standardize histological evaluation (Appendix 1).

Computed tomography acquisition protocol and images analysis

All patients underwent CT scan with a 64-slice multidetector CT scanner (Philips Brilliance 64, Philips, Best, The Netherlands) with a four-phase protocol: unenhanced (UP), corticomedullary (CMP), nephrographic (NP) and excretory phases (EP), i.e., scans respectively before and 30 s, 90 s and 5 min after contrast injection.

An experienced radiologist selected the axial frame showing the largest tumour diameter for each patient's CT scan. Tumours were manually contoured using a dedicated software (Intellispace portal v.8, Philips, Best, The Netherlands) to obtain the region of interest (ROI). The following quantitative features were measured in the ROI: mean, maximum, minimum and standard deviations of the attenuation [measured in Hounsfield unit (HU)]. The following semiquantitative parameters were measured in the ROI: tumour volume, percentage of exophytic growth, tumour-to-psoas ratio on UP scan, tumour-to-kidney ratio on UP, CMP, NP and EP scan, early and late tumour enhancement (defined as the difference between mean attenuation on CMP and mean attenuation on UP scan and the difference between mean attenuation on NP and mean attenuation on UP scan, respectively). The following qualitative features were obtained in the ROI: presence/absence of calcifications, central scar and pseudocapsule, tumour attenuation (hyperdense, isodense, or hypodense relative to adjacent parenchyma), composition (solid or cystic), necrosis, homogeneity [homogeneous or heterogeneous (uniform or mixed attenuation)] (Figure S1).

RNA extraction

Total RNA was extracted from snap frozen ccRCC tissue specimens using TRIzol reagent (Invitrogen), according to manufacturer's instructions. Purity of recovered RNA were determined with a NanoDrop spectrophotometer (ND-1000, NanoDrop Technologies, ThermoFisher). All 6 RNA samples had ~2.0 A260/A280 ratio and 1.8-2.2 A260/A230 ratio. Integrity and concentration of isolated total RNA was assessed with the RNA 6000 Nano LabChip kit using the Agilent 2100 Bioanalyzer (Agilent Technologies). All 6 RNA samples had RIN values >8.

Transcriptomic data analysis

RNA-sequencing was performed by use of Quant Seq 3'mRNA-Seq library prep kit for Illumina® from the previously collected renal tumour specimen stored in our biobank. The prepared libraries were sequenced on Illumina® Next Seq 500 platform, and reads were generated towards poly(A)-tail. Quality control was performed by use of Multi QC platform, and the Fast QC toolkit (Figures S2-S7). Sequences were then mapped to the human genome using the STAR aligner, v. 2.5.3, and annotated according to Gencode basic annotations, version 25. Data generated in this study were deposited in NCBI's Gene Expression Omnibus accessible through GEO Series (accession number GSE133460, link: https://www.ncbi.nlm.nih.gov/geo/query/acc.cgi?acc=GSE133460).

Statistical analyses

Gene expression for each tumour sample was quantified with logarithmic values of Reads Per Kilobase of transcript per Million mapped reads (RPKM).

To assess the heterogeneity of the transcripts among the six samples, several versions of Principal Component Analysis (PCA) were fitted. First, a PCA with all transcripts was performed. Then, a list of 369 out of 406 expressed genes known to be associated with ccRCC from The Cancer Genome Atlas (TCGA) was obtained after excluding 37 genes with a constant expression in our samples, in order to focus on genes really involved in ccRCC and avoid possible confounding variables (Appendix 1) (6). A second PCA with this restricted list was performed. For PCA analyses zero-centred RPKM values were used. Given the small sample size, to account for PCA instability, a bootstrap with 1,000 re-sampling was performed. For each re-sampling, 50 genes with the highest loadings absolute values were extracted. In order to identify pathways and gene ontologies, Enrichment analysis was performed by use of Enrichr (Ma'ayan Laboratory, Mount Sinai Center for Bioinformatics, New York, NY, USA) (21).

Pearson's correlation coefficients were used to assess correlation among radiomic features and between the radiomic features and transcript expression. Adjusted P values were computed by use of Benjamini-Hochberg false discovery rate. Correlation was considered adequate if $\rho<-0.85$ or $\rho>0.85$.

In order to depict correlations between radiomic features and transcripts, a heatmap was used. Moreover, to assess the relationship between radiomic features and transcripts, a hierarchical clustering dendrogram was plotted. Statistical significance of the radiogenomic correlation patterns

Table 1 Patient's characteristics at surgery

Variable	Median [IQR]/n [%]
Age, years	
Median	68
IQR	55–76
Gender	
Male	5 [83]
Female	1 [17]
BMI	
Median	26.2
IQR	22.1–30.1
CCI	
0	3 [50]
1–2	2 [33]
≥3	1 [17]
Preoperative haemoglobin, mg/dL	
Median	14.5
IQR	13.1–15.6
Preoperative eGFR, mL/min/1.73 m^2	
Median	99.5
IQR	84.6–134.2
Preoperative hypertension	
No	3 [50]
Yes	3 [50]
Smoking status	
No smoking history	3 [50]
Active smoker	0 [0]
Former smoker	3 [50]
Clinical tumor size, cm	
Median	4.1
IQR	3.3–4.4
Year of surgery	
Median	2014
IQR	2012–2015
Surgical approach	
Laparotomic	5 [83]
Laparoscopic	0 [0]
Robotic	1 [17]
Affected side	
Left	3 [50]
Right	3 [50]

BMI, body mass index (kg/m^2); CCI, Charlson Comorbidity Index; eGFR, estimated Glomerular Filtration Rates, computed with the Chronic Kidney Disease Epidemiology Collaboration formula for younger patients (<70 years),

was assessed with Mann-Whitney U test, for dichotomic comparison, or with Kruskal-Wallis tests, for multiple comparison.

GraphPad Prism (GraphPad Software La Jolla, CA, USA) and RStudio graphical interface v.0.98 for R software environment v.3.0.2 (http://www.r-project.org) were used for analysis.

Results

Population and tumor characteristics

Median (IQR) age was 68 [55–76] years old (*Table 1*). Five out of 6 patients were male. The median tumour size was 4.1 (3.3–4.4) cm. At histopathological evaluation of the specimens, Fuhrman Grade was 2 in 5 out of 6 specimens while it was 3 in the remaining one; necrosis and lymphoid infiltrates or aggregates were found in half the specimens. Radiologic evidence of intra-tumoral calcifications was found in one case. No central scars were found. The other radiological features are described in Table S1.

RNA sequencing quality control

Quality check for RNA-sequencing was performed. Per base sequence quality of the reads was adequate (Figures S2,S3). The alignment quality was generally good, with almost 80% of reads uniquely mapped on the human genome (Figures S4,S5).

PCA

In the first PCA, using all expressed genes, no clustering was observed between tumour samples (*Figure 1*). When a PCA was ran only against genes significantly associated with

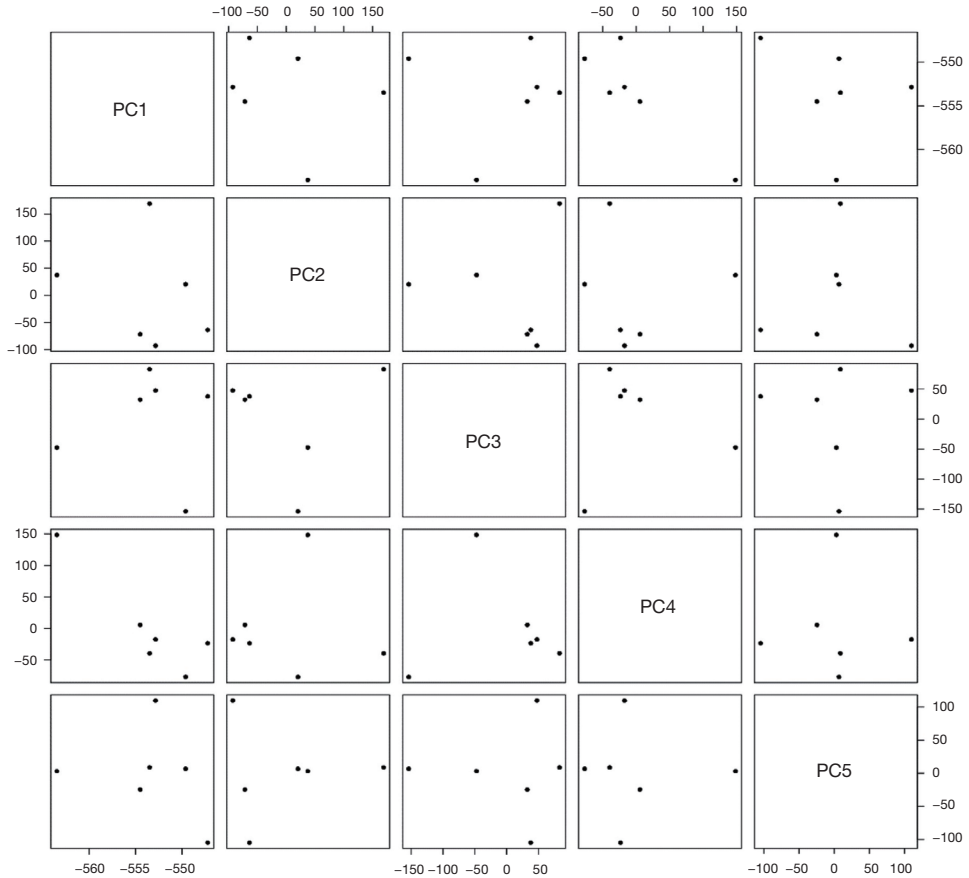

Figure 1 PCA scoreplots for the first five PC, using all expressed genes. Analyses were performed using zero-centred RPKM logarithmic values. The six samples did not cluster in any of the scoreplots. The variances from PC1 to PC5 were 92%, 2.4%, 1.9%, 1.5%, and 1.2%, respectively. PC, principal component; PCA, principal component analysis; RPKM, Reads Per Kilobase of transcript per Million mapped reads.

ccRCC, despite the persistence of high heterogeneity, three tumour samples clustered in PC3 versus PC5 plot, and two in PC1 versus PC5 (*Figure 2*).

Pathways enrichment analysis

Enrichment analysis performed on the top 50 genes with highest loading absolute values in the PCA fitted with transcripts associated with ccRCC showed that the genes driving the clustering in PC3 versus PC5 plot were significantly enriched in pathways related to ECM-receptor interaction pathways, PI3K-Akt signalling pathway, microtubules pathways and calcium homeostasis.

Radiomic features correlation

Among radiomic features, correlation between (I) mean tumour attenuation in CMP and early enhancement (Pearson's correlation ρ=0.99, adjusted P=0.003), (II) mean tumour attenuation in NP and late enhancement (ρ=0.99, P=0.003), and (III) lowest tumour attenuation in CMP and NP (ρ=0.98, P=0.03) was found to be statistically significant.

Radiogenomic correlation

Pearson correlation coefficients were assessed between radiomic features and RPKM values of the ccRCC-associated gene transcripts (data not shown). Using heatmap (*Figure 3*) and dendrogram (*Figure 4*), it was possible to create 4 radiogenomic correlation patterns between expressed genes and radiomic features. In the first pattern, named Radio Genomic Pattern 1 (RGP1), global tumour density and tumour vascular behaviour (i.e., mean tumour attenuation in UP, CMP, NP and early and late tumour

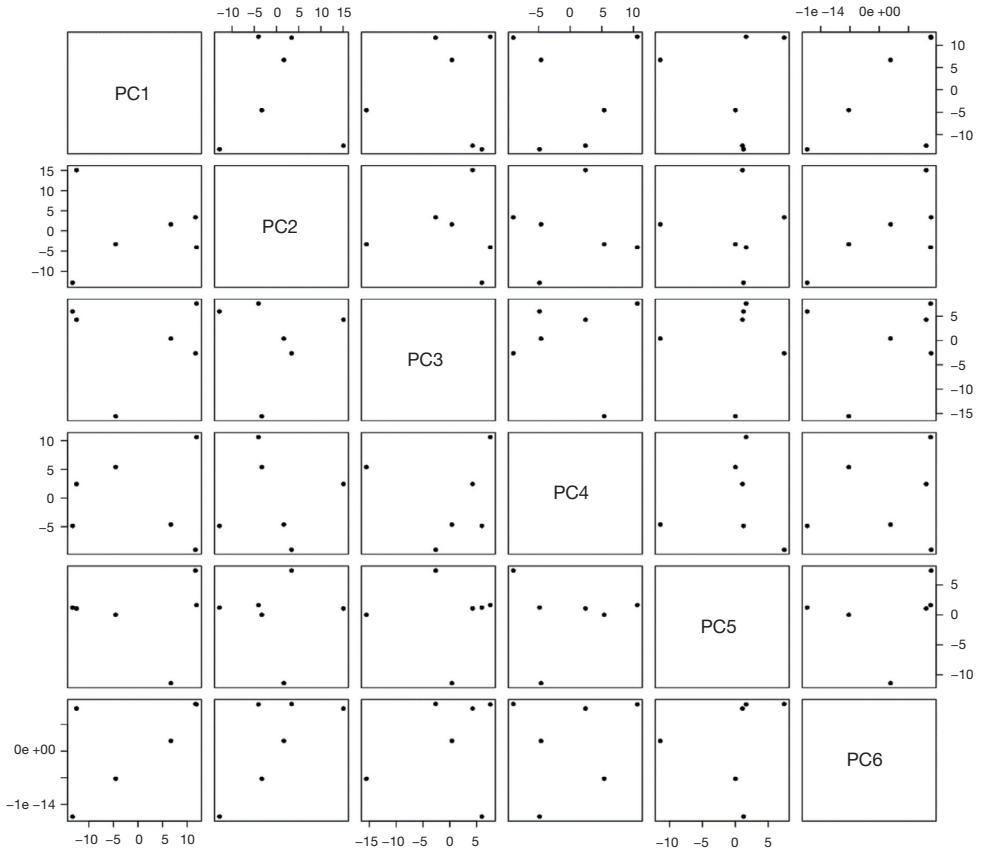

Figure 2 PCA scoreplots for the first six PC restricting the analysis to a list of 369 genes associated with clear cell renal cell carcinoma from TCGA RNAseq and transcriptomic analysis. The list of 369 genes used in the Appendix 1. Analyses were perfomed using zero-centred RPKM logarithmic values. Three samples clustered in PC3 versus PC5 plot, and two tumor samples clustered in PC1 versus PC5 plot. The variances from PC1 to PC6 were 35.1%, 22.4%, 18.6%, 14.1%, 9.9%, and <0.1%, respectively. PC, principal component; PCA, principal component analysis; TCGA, The Cancer Genome Atlas; RPKM, Reads Per Kilobase of transcript per Million mapped reads.

enhancement) were correlated positively with the expression of *VHL*, *COL5A3* and *ANKRD50*, and negatively with *PCDH7*, *PAPOLG* and *PTEN* genes. In the second pattern, named Radio Genomic Pattern 2 (RGP2), hypovascular fat and necrotic components (i.e., lowest tumour attenuation in CMP and NP) were correlated positively with the expression of *PLEC*, *TNR*, *CUL9*, and *UGGT1*, and negatively with *RFC1*, *ESPL1*, *SACS*, *ACVR1B*, *DNAH5*, *KIAA0368*, *ANK3*, *VWA8*, *PHF20*, *USF3*, *DNAH7*, *ARHGAP5*, *SMC3*, *ZMYM1* and *CMYA5* genes. In the third pattern, named Radio Genomic Pattern 3 (RGP3), mean vascularization of kidney and tumour mass (i.e., mean attenuation of the renal cortex in the NP and maximum tumour attenuation in the NP) were correlated positively with the expression *ATM*, and negatively with *PAPOLG* gene. In the fourth pattern, named Radio Genomic Pattern 4 (RGP4), maximum tumour hypervascular areas (i.e., maximum tumour attenuation in the CMP) and kidney-to-tumour attenuation ratio in the CMP were correlated positively with the expression of *CHD9*, *ALMS1*, *SMARCA4*, *GPATCH8*, *ITSN2*, *CDH8*, *KIF21B*, *NCOR1*, *KMT2C* and *SPAG17*, and negatively with *SVEP1* and *LAMA2* genes.

Discussion

Our pilot methodological study was designed to assess the feasibility of a combined radiogenomic approach in the work-up of organ-confined non-metastatic monolateral ccRCC, based on RNA sequencing and radiomic features.

The application of radiomics in RCC is still at a very early stage, with few reports published and a huge

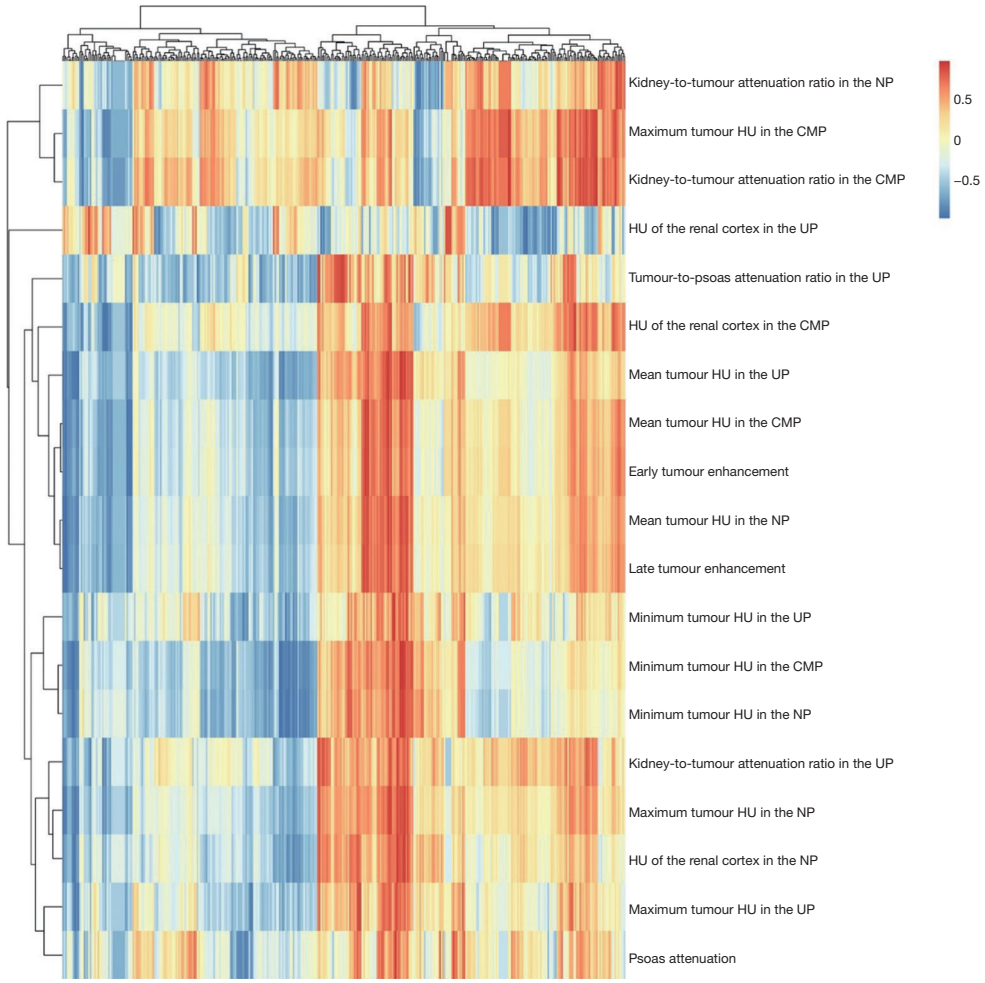

Figure 3 Heatmap showing the correlation between expressed genes and 19 radiomic features. Correlation strength is shown from red to blue, ranging from complete positive to complete negative correlation on the base of Pearson's correlation coefficients. HU, Hounsfield unit; UP, unenhanced phase; CMP, corticomedullary phase; NP, nephrographic phase.

heterogeneity of methodologies applied (19,20). A potential role of radiomics in prediction of RCC subtype, grade and long-term oncologic outcomes has been suggested. Concerns have been raised on the reproducibility of this approach because of use of unstandardized CT-scan protocols in different centres. The main criticisms to radiomics is the lack of a straightforward interpretation of the association between imaging and biological features (15,16). However, studies focusing on the relationship between genomic and radiomic features in different oncological setting are gaining momentum, and recently a review on RCC radiogenomics has been published (22).

In the current pilot study, we investigated the association between RCC transcriptomic and qualitative, semiquantitative and quantitative radiomic features. Initial PCA showed high transcriptomes heterogeneity, as no samples clustered in any of the PCA matrixes. A second PCA was run using a restricted list of 369 ccRCC-associated genes (Appendix 1). In this PCA, heterogeneity was still high, but three sample clustered in the PC3 versus PC5 plot. PC3 and PC5 explained a not negligible portion of the transcriptomic variance (18.6% and 9.9%, respectively).

Enrichment analysis performed on the top 50 genes with highest loading absolute values in the second PCA revealed different pathways and gene ontologies: the three samples clustering in PC3 versus PC5 plot had similar expression of the genes regulating the ECM-receptor interaction pathways, PI3K-Akt signalling pathway, microtubules

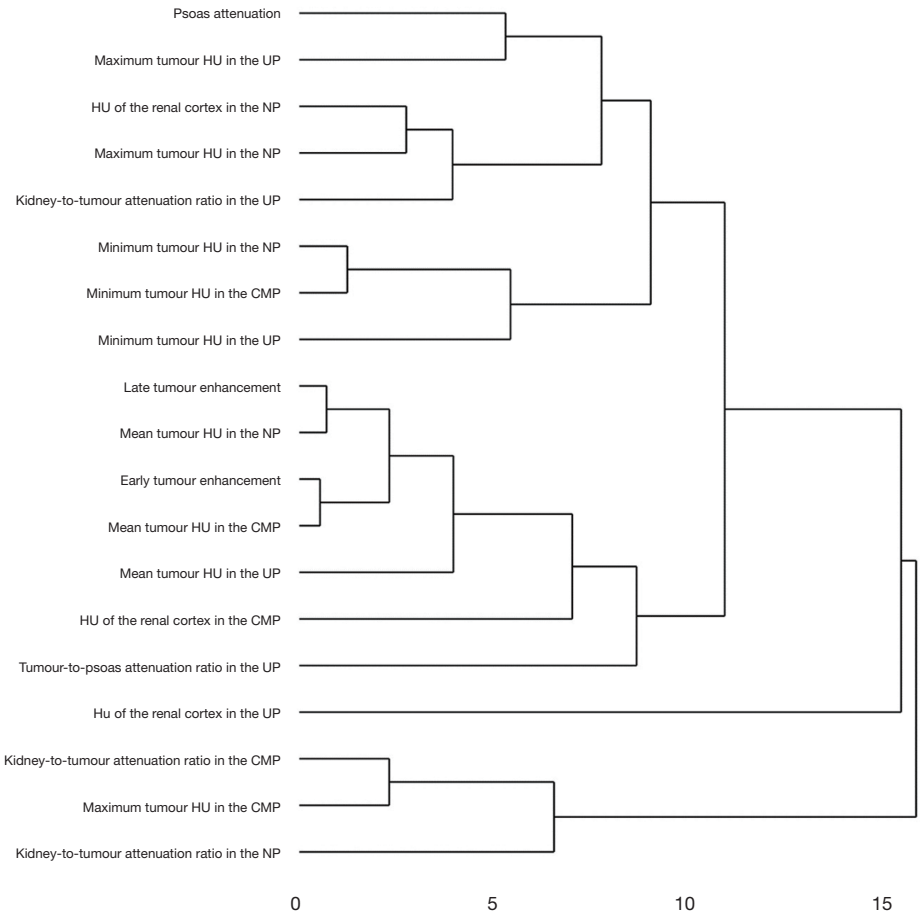

Figure 4 Dendrogram showing hierarchical clustering. Clustering was performed on the base of correlation coefficients between gene expression and radiomic feature. HU, Hounsfield unit; UP, unenhanced phase; CMP, corticomedullary phase; NP, nephrographic phase.

function and calcium homeostasis.

In addition, despite the low numerosity of our study population, we were able to finds correlations between expressed genes and some radiologic features. The radiologic features included in RGP1 showed a strong positive correlation with the expression of *VHL* gene, a key gene in RCC oncogenesis, and *ANKRD50* gene, involved in endosome-to-plasma membrane trafficking and recycling of SNX27-retromer-dependent cargo proteins (23). In RPG1 radiomic features were also positively associated with the expression of *COL5A3* gene, an ubiquitous fibrillar collagen. On the contrary, a strong negative correlation was found between radiomic features and the expression of *PCDH7* gene, whose product is an integral membrane protein involved in cell-cell recognition and adhesion (24), with the expression of *PAPOLG* gene, which encodes a member of the poly(A) polymerase family (25), and with the expression of *PTEN* gene, a tumor suppressor gene whose product antagonizes the PI3K-AKT/PKB signalling pathway and modulates cell cycle progression and cell survival. Of note, RGP1 radiomics features included lesion attenuation and early and late tumour enhancement, which are all radiologic vascular features. VHL and PTEN are frequently mutated in ccRCC, and are usually associated with aggressive tumoral features and neoangiogenesis (26). Expressed genes in RGP2 included cytoskeleton regulatory genes involved in microtubules and ECM function and architecture, protein misfolding pathways and chromosome clustering during mitosis (27-29). Of note, RGP2 radiomic features included hypovascular areas, as for fat, cystic or necrosis areas, where some of the aforementioned genes might play a role (27). In RGP3 the mean contrast enhancement of renal cortex and

of tumor clustered together, suggesting a relation between renal cortical and tumoral vascular features, which might be driven by similar expressed genes. Finally, in RPG4 tumor hypervascular features were related to transcripts for nucleic acid binding, chromatin organization, microtubule motor activity and calcium ion binding (30,31).

This study is not devoid of limitation. A major limitation is the small size of patient's cohort and their strict inclusion criteria. In addition, we were not able to investigate the impact of radiogenomic patterns on oncologic outcomes. Likely, further radiogenomic analyses might yield new evidences on long-term oncologic outcomes according to the different radiogenomic patterns, and the inclusion of radiogenomic data in predictive-prognostic tools might be of key clinical value.

However, with the current study, we demonstrated that radiogenomic approach in ccRCC is methodological feasible.

Conclusions

In this pilot methodological study, in patients with small low-grade organ-confined non-metastatic ccRCC, the transcriptomes of tumor samples were characterized by high heterogeneity. Gene expression was associated with different radiologic features and four main patterns were found, each including different radiomic and transcripts correlates, likely linked by biologic underpinnings. However, further investigations on radiogenomic approaches in ccRCC work-up are needed.

Acknowledgments

Funding: None.

Footnote

Reporting Checklist: The authors have completed the MDAR reporting checklist. Available at https://tau.amegroups.com/article/view/10.21037/tau-21-713/rc

Data Sharing Statement: Available at https://tau.amegroups.com/article/view/10.21037/tau-21-713/dss

Conflicts of Interest: All authors have completed the ICMJE uniform disclosure form (available at https://tau.amegroups.com/article/view/10.21037/tau-21-713/coif). The authors have no conflicts of interest to declare.

Ethical Statement: The authors are accountable for all aspects of the work in ensuring that questions related to the accuracy or integrity of any part of the work are appropriately investigated and resolved. The study was approved by the institutional ethical board of San Raffaele Hospital in Milan (protocol No. URI001-2010 RENE - version 29/08/2007). Informed consent was collected from each patient. The study was conducted in accordance with the principles outlined in the Declaration of Helsinki (as revised in 2013).

References

1. Capitanio U, Montorsi F. Renal cancer. Lancet 2016;387:894-906.
2. Siegel RL, Miller KD, Fuchs HE, et al. Cancer Statistics, 2021. CA Cancer J Clin 2021;71:7-33.
3. Zwirner K, Hilke FJ, Demidov G, et al. Radiogenomics in head and neck cancer: correlation of radiomic heterogeneity and somatic mutations in TP53, FAT1 and KMT2D. Strahlenther Onkol 2019;195:771-9.
4. Zanfardino M, Pane K, Mirabelli P, et al. TCGA-TCIA Impact on Radiogenomics Cancer Research: A Systematic Review. Int J Mol Sci 2019;20:6033.
5. Zhu Z, Albadawy E, Saha A, et al. Deep learning for identifying radiogenomic associations in breast cancer. Comput Biol Med 2019;109:85-90.
6. Cancer Genome Atlas Research Network. Comprehensive molecular characterization of clear cell renal cell carcinoma. Nature 2013;499:43-9.
7. Guo G, Gui Y, Gao S, et al. Frequent mutations of genes encoding ubiquitin-mediated proteolysis pathway components in clear cell renal cell carcinoma. Nat Genet 2011;44:17-9.
8. Dalgliesh GL, Furge K, Greenman C, et al. Systematic sequencing of renal carcinoma reveals inactivation of histone modifying genes. Nature 2010;463:360-3.
9. Brugarolas J. Molecular genetics of clear-cell renal cell

carcinoma. J Clin Oncol 2014;32:1968-76.
10. Motzer RJ, Tannir NM, McDermott DF, et al. Nivolumab plus Ipilimumab versus Sunitinib in Advanced Renal-Cell Carcinoma. N Engl J Med 2018;378:1277-90.
11. Hutson TE, Escudier B, Esteban E, et al. Randomized phase III trial of temsirolimus versus sorafenib as second-line therapy after sunitinib in patients with metastatic renal cell carcinoma. J Clin Oncol 2014;32:760-7.
12. Wei JH, Haddad A, Wu KJ, et al. A CpG-methylation-based assay to predict survival in clear cell renal cell carcinoma. Nat Commun 2015;6:8699.
13. Kapur P, Peña-Llopis S, Christie A, et al. Effects on survival of BAP1 and PBRM1 mutations in sporadic clear-cell renal-cell carcinoma: a retrospective analysis with independent validation. Lancet Oncol 2013;14:159-67.
14. Ljungberg B, Albiges L, Abu-Ghanem Y, et al. European Association of Urology Guidelines on Renal Cell Carcinoma: The 2019 Update. Eur Urol 2019;75:799-810.
15. Lambin P, Leijenaar RTH, Deist TM, et al. Radiomics: the bridge between medical imaging and personalized medicine. Nat Rev Clin Oncol 2017;14:749-62.
16. Avanzo M, Stancanello J, El Naqa I. Beyond imaging: The promise of radiomics. Phys Med 2017;38:122-39.
17. Kickingereder P, Neuberger U, Bonekamp D, et al. Radiomic subtyping improves disease stratification beyond key molecular, clinical, and standard imaging characteristics in patients with glioblastoma. Neuro Oncol 2018;20:848-57.
18. Zhang Y, Oikonomou A, Wong A, et al. Radiomics-based Prognosis Analysis for Non-Small Cell Lung Cancer. Sci Rep 2017;7:46349.
19. Ding J, Xing Z, Jiang Z, et al. CT-based radiomic model predicts high grade of clear cell renal cell carcinoma. Eur J Radiol 2018;103:51-6.
20. Yu H, Scalera J, Khalid M, et al. Texture analysis as a radiomic marker for differentiating renal tumors. Abdom Radiol (NY) 2017;42:2470-8.
21. Kuleshov MV, Jones MR, Rouillard AD, et al. Enrichr: a comprehensive gene set enrichment analysis web server 2016 update. Nucleic Acids Res 2016;44:W90-7.
22. Alessandrino F, Shinagare AB, Bossé D, et al. Radiogenomics in renal cell carcinoma. Abdom Radiol (NY) 2019;44:1990-8.
23. Kvainickas A, Orgaz AJ, Nägele H, et al. Retromer- and WASH-dependent sorting of nutrient transporters requires a multivalent interaction network with ANKRD50. J Cell Sci 2017;130:382-95.
24. Zhou X, Updegraff BL, Guo Y, et al. PROTOCADHERIN 7 Acts through SET and PP2A to Potentiate MAPK Signaling by EGFR and KRAS during Lung Tumorigenesis. Cancer Res 2017;77:187-97.
25. Topalian SL, Kaneko S, Gonzales MI, et al. Identification and functional characterization of neo-poly(A) polymerase, an RNA processing enzyme overexpressed in human tumors. Mol Cell Biol 2001;21:5614-23.
26. Jonasch E, Walker CL, Rathmell WK. Clear cell renal cell carcinoma ontogeny and mechanisms of lethality. Nat Rev Nephrol 2021;17:245-61.
27. Anlar B, Gunel-Ozcan A. Tenascin-R: role in the central nervous system. Int J Biochem Cell Biol 2012;44:1385-9.
28. Lopez J, Tait SW. Killing the Killer: PARC/CUL9 promotes cell survival by destroying cytochrome C. Sci Signal 2014;7:pe17.
29. Daikoku S, Seko A, Son SH, et al. The relationship between glycan structures and expression levels of an endoplasmic reticulum-resident glycoprotein, UDP-glucose: Glycoprotein glucosyltransferase 1. Biochem Biophys Res Commun 2015;462:58-63.
30. van Riel WE, Rai A, Bianchi S, et al. Kinesin-4 KIF21B is a potent microtubule pausing factor. Elife 2017;6:24746.
31. Martínez-Iglesias O, Alonso-Merino E, Aranda A. Tumor suppressive actions of the nuclear receptor corepressor 1. Pharmacol Res 2016;108:75-9.

Cite this article as: Cianflone F, Lazarevic D, Palmisano A, Fallara G, Larcher A, Freschi M, Dell'Antonio G, Scotti GM, Morelli MJ, Ferrara AM, Trevisani F, Cinque A, Esposito A, Briganti A, Tacchetti C, Doglioni C, del Maschio A, de Cobelli F, Bertini R, Salonia A, Montorsi F, Tonon G, Capitanio U. Radiomic and gEnomic approaches for the enhanced DIagnosis of clear cell REnal Cancer (REDIRECt): a translational pilot methodological study. Transl Androl Urol 2022;11(2):149-158. doi: 10.21037/tau-21-713

